Drying Technology

ISSN: 0737-3937 (Print) 1532-2300 (Online) Journal homepage: http://www.tandfonline.com/loi/ldrt20

Modeling of Fertilizer Drying in Roto-Aerated and Conventional Rotary Dryers

E. B. Arruda , F. S. Lobato , A. J. Assis & M. A. S. Barrozo

To cite this article: E. B. Arruda , F. S. Lobato , A. J. Assis & M. A. S. Barrozo (2009) Modeling of Fertilizer Drying in Roto-Aerated and Conventional Rotary Dryers, Drying Technology, 27:11, 1192-1198, DOI: 10.1080/07373930903263129

To link to this article: https://doi.org/10.1080/07373930903263129

Published online: 16 Oct 2009.

Drying Technology, 27: 1192–1198, 2009

ISSN: 0737-3937 print/1532-2300 online
DOI: 10.1080/07373930903263129

Taylor & Francis
Taylor & Francis Group

Modeling of Fertilizer Drying in Roto-Aerated and Conventional Rotary Dryers

E. B. Arruda, F. S. Lobato, A. J. Assis, and M. A. S. Barrozo
Federal University of Uberlândia, Chemical Engineering School, Uberlândia, MG, Brazil

Conventional rotary dryers are equipped with flights placed parallel along the length of the shell to promote a rain of solids across the dryer section. In the roto-aerated dryer the hot air flows through the particles that run on the bottom of the drum through a series of mini-pipes and there is no cascading. This study analyzed heat and mass transfer modeling between the air and the fertilizer particles in conventional rotary and roto-aerated dryers, as well as the simulation results with the experimental data. A good agreement between the simulated and experimental results was obtained for the two rotary dryer configurations analyzed.

Keywords Modeling; Rotary dryer; Roto-aerated dryer

INTRODUCTION

Drying, one of the most energy-intensive operations, is of great importance in the fertilizer industry. Despite its importance, in many cases the design and operation of dryers is done according to empiricism, based on the experience of engineers.[1]

Rotary dryers are often used in fertilizer industries. The conventional rotary dryer consists basically of a long cylindrical shell inclined at a small angle to the horizontal and fitted with internal flights to cascade solid material through a concurrent or countercurrent gas stream.[2] Wet feed is introduced into the upper end of the dryer and the dried product withdrawn at the lower end. The length of the drum varies from four to ten times its diameter, which can be 0.2 to more than 3 m wide.[1]

As the dryer rotates, the solids are picked up by the flights and are conveyed for a certain distance around the periphery before dislodging and falling back as a raining curtain through a hot air stream. Thus, in conventional cascading rotary dryers, the particulate material mostly dries during the falling period.[3] The movement of particles in conventional rotary dryers depends on flight design.[4,5] The performance of rotary dryers is dictated by three important transport phenomena, namely, solids transportation,[6–10] heat, and mass transfer. The ability to estimate each of these transport mechanisms is essential for proper design and operation of rotary dryers.[11]

The literature presents some drying models for conventional rotary dryers based on the application of mass and energy balance equations for both solid and fluid phases.[12–17] This approach requires constitutive equations for the heat transfer coefficients, drying kinetics, equilibrium moisture content, and fluid dynamic characteristics.

In order to improve drying efficacy, another version of the rotary dryer, known as a roto-fluidized dryer or, more accurately, roto-aerated dryer, was evaluated by Lisboa[18] and Arruda.[19] This dryer configuration presents as its major characteristic an aerated system consisting of a central pipe (surrounded by the drum) from which a series of mini-pipes conducts the hot air directly to the particle bed that is flowing at the bottom of the surrounding drum (without flights). Figure 1 shows a schematic diagram of air distribution in this novel dryer.

In the roto-aerated dryer, the gas-particle contact is more effective and occurs as long as the solid remains in the dryer, different from the cascading conventional dryer where this contact occurs mostly during the time that the particles are falling from the flights. This fact allows for a reduction of the particle residence time with a subsequent increase in the processing capacity, as observed by Lisboa.[18] Moreover, greater transfer coefficients of mass and energy were observed in preliminary studies, resulting in increased efficacy of the roto-aerated dryer in relation to the conventional equipment. These factors motivated a more detailed study, performed by Arruda,[19] to identify and quantify the performance differences between the conventional and the roto-aerated dryers.

The aim of this work is to study the modeling of the heat and mass transfer between the air and the particles of superphosphate fertilizer in conventional rotary and roto-aerated dryers, as well as to compare the simulation results with experimental data. The utilized model is based on the mass and energy balances performed on infinitesimal volume elements in the rotary dryers operating at steady state. The constitutive equations were obtained in our previous study.[19]

Correspondence: M. A. S. Barrozo, Federal University of Uberlândia, Chemical Engineering School, Block K, Campus Santa Mônica, CEP 38400-902, Uberlândia, MG, Brazil; E-mail: masbarrozo@pesquisador.cnpq.br

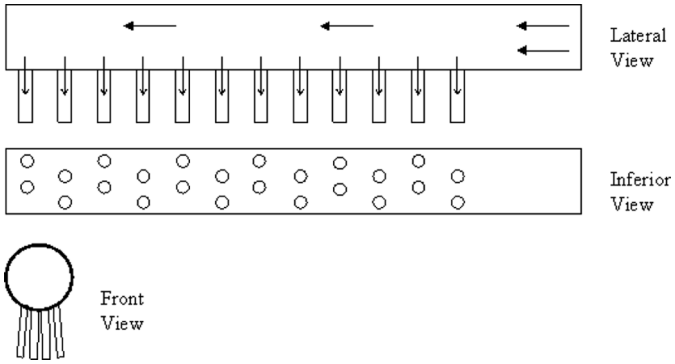

FIG. 1. Schematic diagram of air distribution in the roto-aerated dryer.

EQUATIONS

The load of materials into the flights depends on its angular position at the drum and the intrinsic characteristics of the material, such as dynamic angle of repose, particle size (d_P), and the dynamic friction coefficient. This load can be calculated using the equations proposed by Revol et al.[20] for flights with angular geometry. These equations were previously tested and validated by Arruda.[19]

Simultaneous Transfer of Mass and Energy in Rotary Dryers

The system was modeled by applying mass and energy balances for both solid and fluid phases. The modeling approach considers the fluid dynamic characteristics of the dryer, as well as the intrinsic properties of the material, equilibrium moisture, and drying kinetics. The operations of both rotary dryers were assumed to be in a steady state. Figure 2 shows the scheme of the infinitesimal volume element of a conventional rotary dryer operating at a countercurrent flow.

In the formulation of this model, the following assumptions were made:

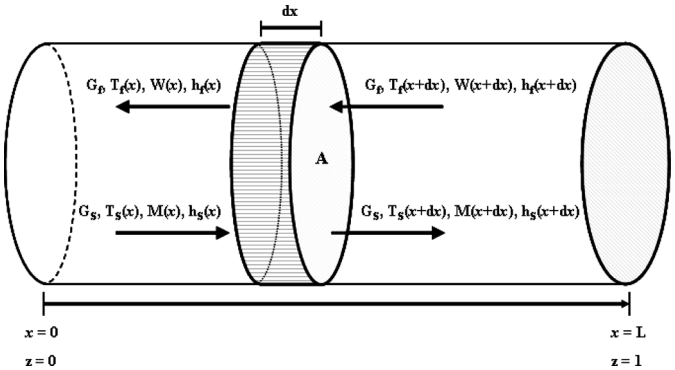

FIG. 2. Schematic of the infinitesimal volume element of the rotary dryer operating at countercurrent flow.

- The particle velocity through the drum is constant.
- The drying rate is evaluated in each infinitesimal volume element volume of the dryer;
- Grain shape and physical properties do not change during drying;
- The initial conditions of solid feeding flow rate, air and solid temperature, air humidity and solid moisture are known.

The equation system from the balances of mass and energy between drying gas and particulate material is presented next, where z is the nondimensional length, given by the proportion between a given position (x) and the total length of the dryer (L).

$$\frac{dW}{dz} = -\frac{R_w H^*}{G_f} \tag{1}$$

$$\frac{dM}{dz} = -\frac{R_w H^*}{G_S} \tag{2}$$

$$\frac{dT_f}{dz} = \frac{\left[\begin{array}{l} U_{va} V(T_f - T_S) + R_w H^*(\lambda + Cp_v T_f) \\ + U_P \pi D L(T_f - T_{amb}) \end{array}\right]}{G_f(Cp_f + WCp_v)} \tag{3}$$

$$\frac{dT_S}{dz} = \frac{\left[\begin{array}{l} U_{va} V(T_f - T_S) + R_w H^* Cp_l T_S \\ - R_w H[\lambda + Cp_v(T_f - T_S)] \end{array}\right]}{G_S(Cp_S + MCp_l)} \tag{4}$$

The system of differential equations of the model should be resolved simultaneously for the four variables involved, considering the contour conditions that follow:

$$W(L) = W_0; \quad M(0) = M_0; \quad T_f(L) = T_{f0}; \quad T_S(0) = T_{S0}.$$

Drying in conventional cascading rotary dryers occurs mostly during the time in which the particles are falling from the flights; that is, they are in contact with the drying air, which corresponds to only a fraction of the residence time.[21] This fraction refers to the effective contact time between the solid and drying air (f_{tef}) and can be evaluated by the relation between the average falling time of the particle and total time of a cycle. This, in turn, corresponds to the time spent from material collection by the flight until its return to the particle bed on the bottom of the drum. This fraction can be evaluated by Eq. (5), where the total number of cycles (N_{Ci}) is given by Eq. (6), and the effective contact time gas-particle (t_{ef}) by Eq. (7). The total solids load in the dryer (H^*) is given by Eq. (8).

$$f_{tef} = \frac{\bar{t}_q}{\bar{t}_{Ci}} \times \frac{N_{Ci}}{N_{Ci}} = \frac{N_{Ci}\bar{t}_q}{\bar{\tau}} \tag{5}$$

$$N_{Ci} = \frac{L}{l} = \frac{L}{\overline{\overline{Y_q} sen(\alpha)}} \quad (6)$$

$$t_{ef} = f_{tef} \times \overline{\tau} \quad (7)$$

$$H^* = \overline{\tau} \times G_S \quad (8)$$

For the conventional rotary dyer, the effective contact time gas-particle (t_{ef}) substitutes the time t in the computation of the drying rate. In the roto-aerated dryer this effective contact time is equal to the residence time itself; that is, the fraction of effective time (f_{tef}) is equal to one.

Constitutive Equations

Equilibrium Moisture

Based on experimental data of equilibrium moisture content of the simple superphosphate fertilizer, Arruda[19] performed a statistic study of discriminating rival models and concluded that the modified Halsey correlation[22] best adjusted his experimental data. The modified Halsey's equation with the parameters estimated by Arruda[19] for the superphosphate fertilizer is presented next.

$$M_{eq} = \left(\frac{-\exp(-0.045 T_S - 2.08)}{\ln(RH)} \right)^{\frac{1}{1.435}} \quad (9)$$

Drying Kinetics

Based on the experimental study performed in a thin layer, Arruda[19] concluded that the best correlation to represent the drying kinetics of the fertilizer was Page's equation.[23] Page's equation with the parameters estimated by Arruda[19] for simple superphosphate is presented subsequently:

$$MR = \frac{M - M_{eq}}{M_0 - M_{eq}} = \exp\left[-0.431 \exp\left(\frac{-121.845}{T_f} \right) t^{0.392} \right] \quad (10)$$

Heat Transfer Coefficients

The best correlations for global volumetric heat transfer coefficient (U_{va}) and for the lost heat through the wall coefficient (U_P) also were determined by Arruda.[19] These equations with the parameters estimated in this previous work are

$$U_{va} = 3.535 G_f^{0.289} G_S^{0.541} \quad (11)$$

$$U_P = 0.227 G_f^{0.879} \quad (12)$$

MATERIALS AND METHODS

The particles in this study were fertilizer in the form of simple superphosphate granules (SSPG) of 2.45 mm Sauter mean diameter, 1100 kg/m^3 particle density, and 0.245 kcal/kg°C heat capacity, with a initial moisture contents between 0.12 and 0.15 kg water/kg dry solid. The dynamic coefficient of friction determined by Arruda[19] for this material was 0.984.

Experimental Setup Description

Figure 3 shows a schematic view of the experimental apparatus that consists of a 7.5 hp blower, an air heating system with electrical resistances controlled by a Variac, the rotary dryer (conventional or roto-aerated), and a transporting belt for the solids feeding mounted under a silo of moist fertilizer. The hot air enters the conventional cascading rotary dryer in countercurrent flow with the solids. The rotary dryer was 1.5 m long and 0.3 m wide and was built to allow changes in the drum's inclination and rotation and to operate with any number and types of flights or adapted for the roto-aerated configuration.

Experimental Conditions

The experimental trials were performed with the best configurations determined by Arruda[19] for the conventional and roto-aerated dryers. The conventional rotary dryer was equipped with three-segmented angular flights. This choice[19] was due to the fact that this type of flight promotes a more homogeneous cascading through the transversal section of the rotary dryer, thus promoting a better spreading of the material and, consequently, a better contact between the falling particles and the drying air. The flights had the following dimensions: first segment = 0.02 m, second and third segment = 0.007 m; the length of the flights was 1.5 m, with an angle of 135° between segments.

The most effective configuration for the roto-aerated dryer, among several tested by Arruda,[19] was the one using a fixed 10-cm-diameter central pipe (surrounded by the drum), from which fifty-six 0.9-cm-diameter mini-pipes derived, disposed as shown in Fig. 1. The length of the mini-pipes was adjusted in such a way that they remained as close to the bottom of the surrounding drum as possible.

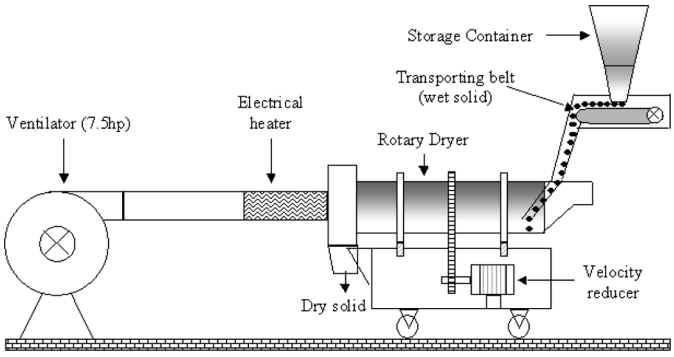

FIG. 3. Schematic of the experimental apparatus.

TABLE 1
Experimental design

Experiment	v_f (m/s)	T_f (°C)	G_S (kg/min)
1	1.5	75	0.8
2	1.5	75	1.2
3	1.5	95	0.8
4	1.5	95	1.2
5	3.5	75	0.8
6	3.5	75	1.2
7	3.5	95	0.8
8	3.5	95	1.2
9	1.09	85	1
10	3.91	85	1
11	2.5	70.9	1
12	2.5	99.1	1
13	2.5	85	0.72
14	2.5	85	1.28
15	2.5	85	1

Experimental Design

The experimental conditions (see Table 1) were chosen by a central composed experimental design.[24] Measurements of solids moisture and temperature were performed through the length of the drum using a probe containing a collector mounted on its tip with a copper-constantan thermocouple. Solids moisture content was determined by the stove method (24 h at 105 ± 2°C). Air and solids temperatures were measured using a copper-constantan thermocouple.

RESULTS AND DISCUSSION

The resolution of the differential equations system was obtained by the technique of normal collocation with 10 placement points for the fourth-order polynomial approximation, using the subroutine bvp4c of the software Matlab®. The relative tolerance used was 10^{-6}. The simulated results of fertilizer moisture distribution, as well as the air and solid temperature profiles along the length of the both rotary dryers, were compared with the respective experimental data.

Conventional Rotary Dryer

Figures 4 to 6 show typical results of the comparisons between experimental profiles and those computed by the model for the conventional dryer under optimum operational conditions. A good agreement between the simulated profiles and those obtained experimentally for the conventional rotary cascading dryer can be observed in these results, with a slight overprediction for the solid temperature. The good agreement between simulated and experimental results was also observed in the other condition of the experimental design (Table 1).

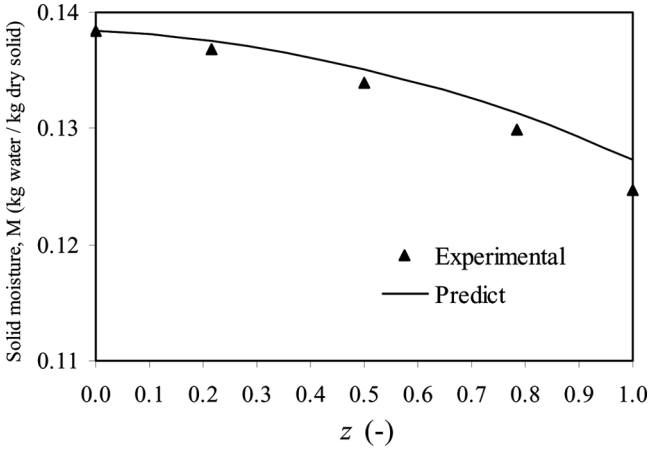

FIG. 4. Experimental and simulated results of the solids moisture profile for the conventional rotary dryer operating in the conditions of test 2: $v_{AR} = 1.5$ m/s; $T_f = 75$°C; $G_S = 1.2$ kg/min.

Figures 7 to 9 show the experimental and simulated results, obtained at the exit of the dryer, respectively, for the solids moisture content, solids and air temperatures, for each experiment of this study (see conditions in Table 1). The average deviation of the simulation results in relation to experimental data for the solids moisture was 7.7%, 12.8% for solids temperature, and 4.6% for air temperature. Therefore, it can be said that the simulation results well matched with the experimental data for the conventional rotary dryer.

Roto-Aerated Dryer

The experimental data and those computed by the model for solids moisture distribution, as well as solid and air temperatures along the length of the roto-aerated dryer, are shown in Figs. 10 to 12 for the conditions of the test 3 (see Table 1), where a good agreement between

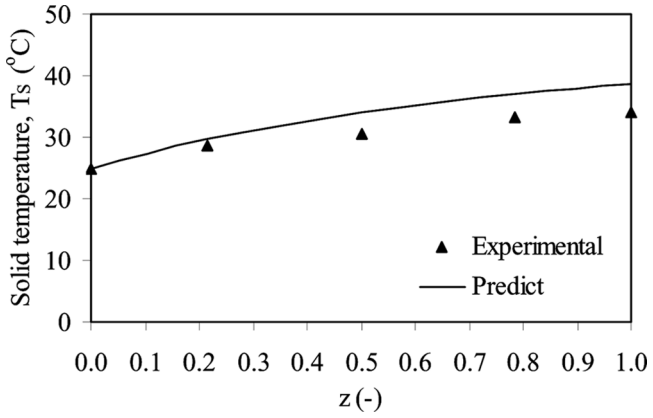

FIG. 5. Experimental and simulated results of the solids temperature for the conventional rotary dryer operating in the conditions of test 2: $v_{AR} = 1.5$ m/s; $T_f = 75$°C; $G_S = 1.2$ kg/min.

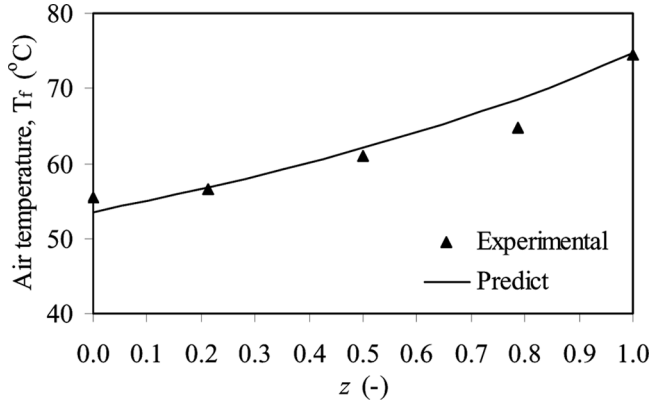

FIG. 6. Experimental and simulated results of the fluid temperature for the conventional rotary dryer operating in the conditions of test 2: $v_{AR} = 1.5\,\text{m/s}$; $T_f = 75°\text{C}$; $G_S = 1.2\,\text{kg/min}$.

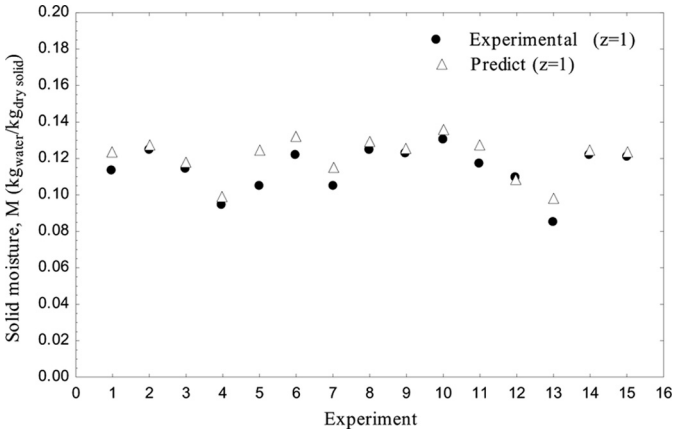

FIG. 7. Experimental and simulated results for the solids moisture content at the exit of the conventional dryer for each experiment (see conditions in Table 1).

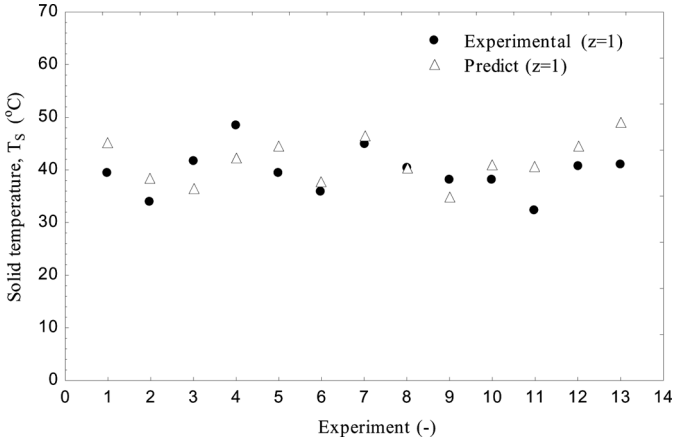

FIG. 8. Experimental and simulated results for the solids temperature at the exit of the conventional rotary dryer for each experiment (conditions in Table 1).

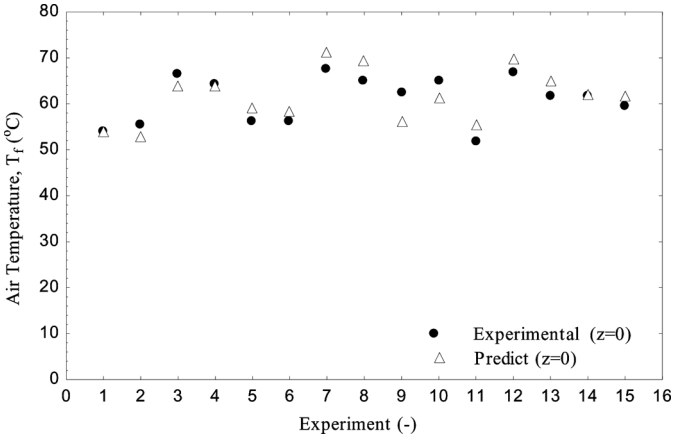

FIG. 9. Experimental and simulated results for the fluid temperature at the exit of the conventional rotary dryer for each experiment (conditions in Table 1).

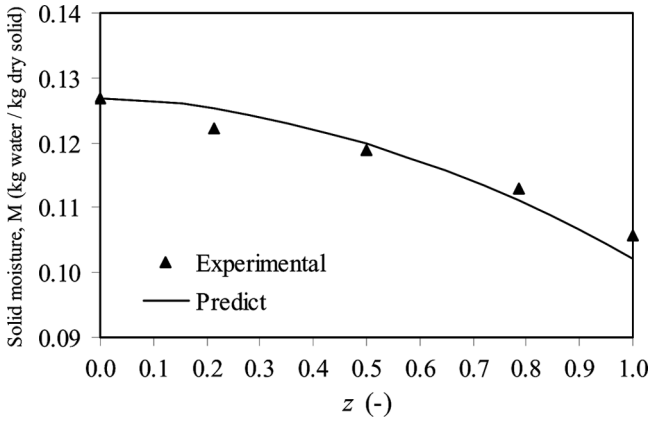

FIG. 10. Experimental and simulated results of the solids moisture profile for the roto-aerated dryer operating in the conditions of test 3: $v_{AR} = 1.5\,\text{m/s}$; $T_f = 75°\text{C}$; $G_{SU} = 0.8\,\text{kg/min}$.

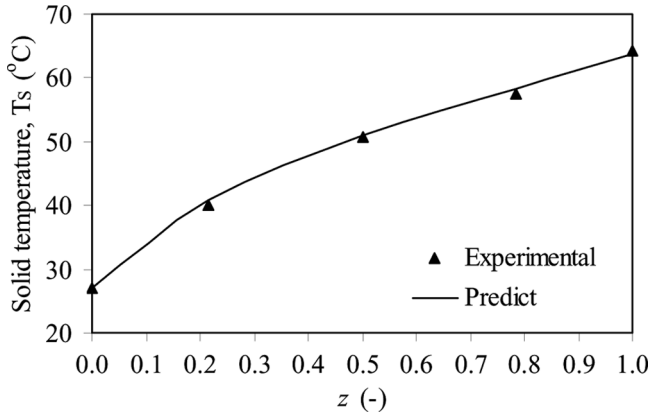

FIG. 11. Experimental and simulated results of the solids temperature profile for the roto-aerated dryer operating in the conditions of test 3: $v_{AR} = 1.5\,\text{m/s}$; $T_f = 75°\text{C}$; $G_{SU} = 0.8\,\text{kg/min}$.

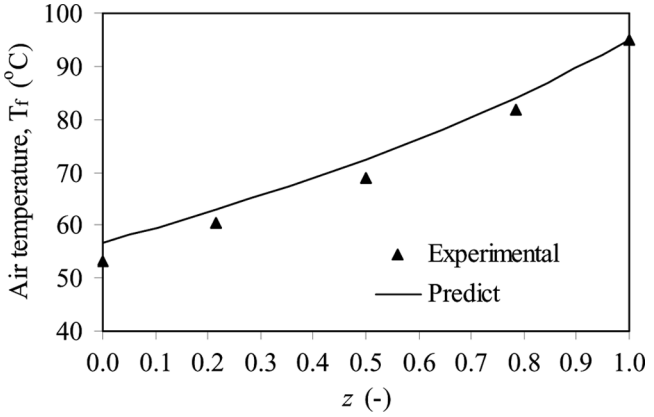

FIG. 12. Experimental and simulated results of the air temperature profile for the roto-aerated dryer operating in the conditions of test 3: $v_{AR} = 1.5\,m/s$; $T_f = 75°C$; $G_{SU} = 0.8\,kg/min$.

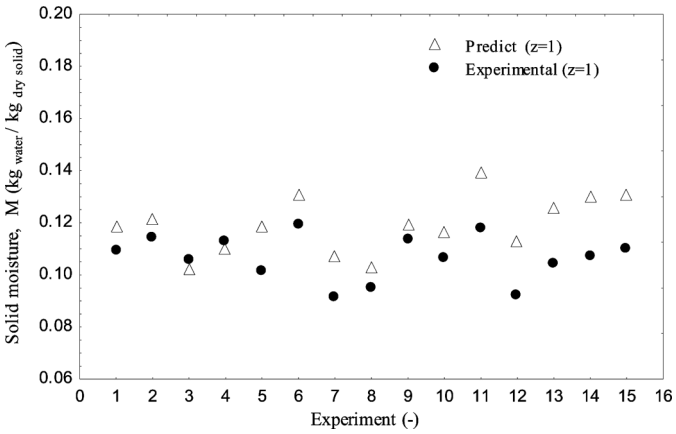

FIG. 13. Experimental and simulated results for the solids moisture content at the exit of the roto-aerated dryer for each experiment (see conditions in Table 1).

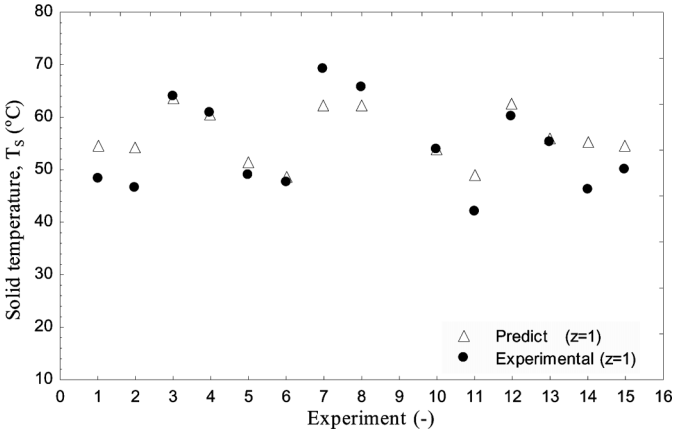

FIG. 14. Experimental and simulated results for the solids temperature at the exit of the roto-aerated rotary dryer for each experiment (conditions in Table 1).

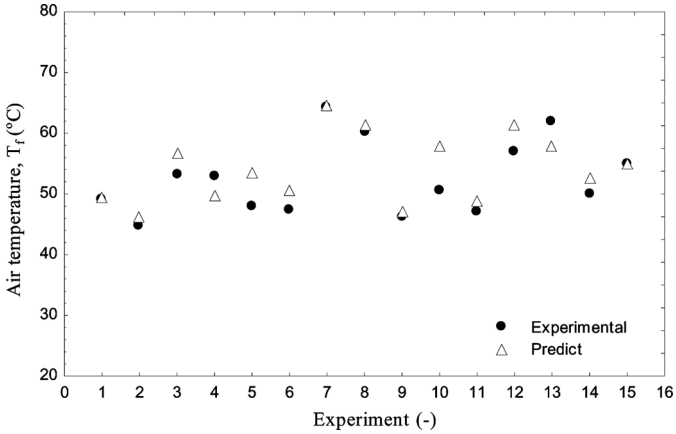

FIG. 15. Experimental and simulated results for the air temperature at the exit of the roto-aerated rotary dryer for each experiment (conditions in Table 1).

the simulated and experimental results is observed. The trend observed in these figures also was observed in the other condition of the experimental design.

Figures 13 to 15 show the comparison between the simulated and experimental results at the exit of the roto-aerated dryer for all experiments presented in Table 1. The average deviation observed in relation to the experimental data was 12.4% for the solids moisture content, 7.4% for the solids temperature, and 5.2% for the air temperature. Therefore, it can be stated that the model proposed in this study was also capable of adequately predicting the drying performance in this novel dryer. It is important to highlight that in the simulation approach utilized here the parameters of the constitutive equations were estimated in specific studies of drying kinetics, equilibrium moisture content, and heat transfer coefficients.[19]

CONCLUSIONS

From the mass and energy balances performed over infinitesimal volume elements in the rotary dryer, a mathematical model, consisting of a system of differential equations able to adequately describe air and solids moisture and temperature distribution along the length of both conventional and roto-aerated dryers, was used in this work.

The average deviation of the simulation results in relation to experimental data, for the conventional rotary dryer, was 7.7% for the solids moisture content, 12.8% for the solids temperature, and 4.6% for the air temperature. For the roto-aerated dryer, the average deviation was 12.4% for the solids moisture content, 7.4% for the solids temperature, and 5.2% for the air temperature.

Therefore, it can be stated that the methodology utilized in this work—i.e., the drying model with the parameters obtained in specific studies—can be used in optimization

and project studies of rotary dryers, both conventional and roto-aerated.

NOMENCLATURE

D	Dryer diameter (m)
d_p	Particle diameter (m)
f_{tef}	Effective time factor
G	Mass flow rate (kg/min)
H^*	Dryer total load (kg)
L	Dryer length (m)
M	Solid moisture ($kg_{water}/kg_{dry\ solid}$)
MR	$=\frac{M-M_{eq}}{M_0-M_{eq}}$ non dimensional moisture
N_{Ci}	Total number of cycles
N_R	Rotation velocity (rpm)
RH	Air relative humidity
R_W	Drying rate (min^{-1})
T	Temperature (°C)
t	Time (s)
U_P	Coef. of heat lost ($kWm^{-2\circ}C^{-1}$)
U_{va}	Global volumetric heat transfer coefficient ($kWm^{-3\circ}C^{-1}$)
W	Air absolute humidity ($kg_{water}/kg_{dry\,air}$)
x	Position along the dryer (m)
$\overline{Y}_q$	Average fall height (m)
z	$=x/L$, non dimensional length

Greek Symbols

α	Dryer inclination (°)
λ	Latent heat of pure water vaporization ($kJ\,kg^{-1}$)
$\overline{\tau}$	Average residence time (s)

Subscripts

amb	Environment
ef	Effective
eq	Equilibrium
f	Fluid
l	Liquid
s	Solid
su	Moist solid
v	Vapor

ACKNOWLEDGEMENT

The authors are thankful to FAPEMIG and CNPq for the financial support.

REFERENCES

1. Lisboa, M.H.; Vitorino, D.S.; Delaiba, W.B.; Finzer, J.R.D.; Barrozo, M.A.S. A study of particle motion in rotary dryer. Brazilian Journal of Chemical Engineering **2007**, *24* (3), 265–374.
2. Sheehan, M.E.; Britton, P.F.; Schneider, P.A. A model for solids transport in flighted rotary dryers based on physical considerations. Chemical Engineering Science **2005**, *60*, 4171–4182.
3. Papadakis, S.E.; Langrish, T.A.G.; Kemp, I.C.; Bahu, R.E. Scale-up of cascading rotary dryers. Drying Technology **1994**, *12* (1), 259–277.
4. Baker, C.G.J. The design of flights in cascading rotary dryers. Drying Technology **1988**, *6*, 631–653.
5. Driver, J.; Hardin, M.T.; Howes, T.; Palmer, G. Effect of lifter design on drying performance in rotary dryers. Drying Technology **2003**, *21* (2), 369–381.
6. Cao, W.F.; Langrish, T.A.G. Comparison of residence time models for cascading rotary dryers. Drying Technology **1999**, *17* (4&5), 825–836.
7. Renaud, M.; Thibault, J.; Trusiak, A. Solids transportation model of an industrial rotary dryer. Drying Technology **2000**, *18* (4&5), 843–865.
8. Shahhosseini, S.; Cameron, I.T.; Wang, F.Y. A simple dynamic model for solid transport in rotary dryers. Drying Technology **2000**, *18* (4&5), 867–886.
9. Song, Y.; Thibault, J.; Kudra, T. Dynamic characteristics of solids transportation in rotary dryers. Drying Technology **2003**, *21* (5), 775–773.
10. Britton, P.F.; Sheehan, M.E.; Schneider, P.A. A physical description of solids transport in flighted rotary dryers. Powder Technology **2006**, *165*, 153–160.
11. Krokida, M.K.; Maroulis, Z.B.; Kremalis, C. Process design of rotary dryers for olive cake. Drying Technology **2002**, *20* (4&5), 771–788.
12. Kemp, I.C.; Oakley, D.E. Simulation and scale-up of pneumatic conveying and cascading rotary dryers. Drying Technology **1997**, *15*, 1699–1710.
13. Cao, W.F.; Langrish, T.A.G. The development and validation of a system model for a countercurrent cascading rotary dryer. Drying Technology **2000**, *18* (1&2), 99–115.
14. Zabaniotou, A.A. Simulation of forestry biomass drying in a rotary dryer. Drying Technology **2000**, *18* (7), 1415–1431.
15. Iguaz, A.; Esnoz, A.; Martinez, G.; López, A.; Vírseda, P. Mathematical modeling and simulation for the drying process of vegetable wholesale by-products in a rotary dryer. Journal of Food Engineering **2003**, *59*, 151–160.
16. Xu, Q.; Pang, S. Mathematical modeling of rotary drying of woody biomass. Drying Technology **2008**, *26*, 1344–1350.
17. Lobato, F.S.; Steffen, V., Jr.; Arruda, E.B.; Barrozo, M.A.S. Estimation of drying parameters in rotary dryers using differential evolution. Journal of Physics: Conference Series **2008**, *135*, 1–8.
18. Lisboa, M.H. *A Study of Fertilizer Drying in Rotary Dryers*; MSc thesis, Uberlândia-Brazil, Federal University of Uberlândia, 2005.
19. Arruda, E.B. *Comparison of the Performance of the Roto-Fluidized Dryer and Conventional Rotary Dryer*; PhD thesis, Uberlândia-Brazil, Federal University of Uberlândia, 2006.
20. Revol, D.; Briens, C.L.; Chabagno, J.M. The design of flights in rotary dryers. Powder Technology **2001**, *121*, 230–238.
21. Baker, C.G.J. Cascading rotary dryers. In *Advances in Drying*; Mujumdar, A.S., Ed.; Hemisphere: New York, 1983; 1–51.
22. Osborn, G.S.; White, G.M.; Sulaiman, A.H.; Welton, L.R. Predicting equilibrium moisture proportions of soybeans. Transactions of the ASAE **1989**, *32* (6), 2109–2113.
23. Page, G.E. *Factors Influencing the Maximum Rates of Air Drying Shelled Corn in Thin-Layer*; MSc thesis, Purdue University, West Lafayette, IN, 1949.
24. Box, M.J.; Hunter, W.G.; Hunter, J.S. *Statistics for Experiments: An Introduction to Design, Data Analysis and Model Building*; John Wiley & Sons; New York, 1978.